Electronic Supplementary Information for:

High-performance organic solar cells based on polymer donor/small molecule donor/nonfullerene acceptor ternary blends

Shuixing Dai,[a] Sreelakshmi Chandrabose,[b] Jingming Xin,[c] Tengfei Li,[a] Kai Chen,[b] Peiyao Xue,[a] Kuan Liu,[a] Ke Zhou,[c] Wei Ma,[c] Justin M. Hodgkiss[b] and Xiaowei Zhan[a,*]

[a] Department of Materials Science and Engineering, College of Engineering, Key Laboratory of Polymer Chemistry and Physics of Ministry of Education, Peking University, Beijing 100871, China, E-mail address: xwzhan@pku.edu.cn

[b] MacDiarmid Institute for Advanced Materials and Nanotechnology, School of Chemical and Physical Sciences, Victoria University of Wellington, Wellington 6010, New Zealand

[c] State Key Laboratory for Mechanical Behavior of Materials, Xi’an Jiaotong University, Xi’an 710049, China

Materials. All the solvents and chemical reagents used were obtained commercially and were used without further purification. TR and PTB7-Th (M_n = 53k, M_w = 120k, and M_w/M_n = 2.27) were purchased from Solarmer Materials Inc. and 1-Material Inc., respectively. FOIC was synthesized according to our published procedure.[1]

Measurements. UV-vis absorption spectra were recorded using a Jasco V-570 spectrophotometer in thin films (on a quartz substrate). Photoluminescence spectra were measured for PTB7-Th, TR neat films and PTB7-Th/TR blended films (spin-coated on a quartz substrate) by using a FLS980 lifetime and steady state spectrometer. The nanoscale morphology of the blends was observed employing a Multimode 8 scanning probe microscopy (Bruker) in the tapping mode.

Fabrication and characterization of OSCs. ITO glass (sheet resistance = 15 $\Omega\ \square^{-1}$) was precleaned in an ultrasonic bath with acetone and isopropanol. ZnO layer was spin coated at 4000 rpm onto the ITO glass from ZnO precursor solution (a mixture of zinc acetate dehydrate (100 mg), 2-methoxyethanol (973 μL) and ethanolamine (28.29 μL) stirred overnight), and then baked at 200 °C for 30 min. A donor: FOIC mixture (10 mg mL^{-1} in total) in chloroform was spin coated at 1300 rpm on the ZnO layer to form a photoactive layer. The MoO_3 layer (*ca.* 5 nm) and Ag (*ca.* 80 nm) were successively evaporated onto the surface of the photoactive layer under vacuum (*ca.* 10^{-5} Pa). The active area of the device was *ca.* 4 mm^2. The *J–V* curve was measured using a computer-controlled B2912A Precision Source/Measure Unit (Agilent Technologies). An XES-70S1 (SAN-EI Electric Co., Ltd.) solar simulator (AAA grade, 70 × 70 mm^2 photobeam size) coupled with AM 1.5 G solar spectrum filters was used as the light source, and the optical power at the sample was 100 mW cm^{-2}. A 2 × 2 cm^2 monocrystalline silicon reference cell (SRC-1000-TC-QZ) was purchased from VLSI Standards Inc. The EQE spectrum was measured using a Solar Cell Spectral Response

Measurement System QE-R3011 (Enlitech Co., Ltd.). The light intensity at each wavelength was calibrated using a standard single crystal Si photovoltaic cell.

GIWAXS characterization. GIWAXS measurements were performed at beamline 7.3.3 [2] at the Advanced Light Source (ALS). Samples were prepared on Si substrates using identical blend solutions as used in OSC devices. The 10 keV X-ray beam was incident at a grazing angle of 0.11°–0.15°, which maximized the scattering intensity from the samples. The scattered X-rays were detected using a Dectris Pilatus 2M photon counting detector.

Resonant soft X-ray scattering. R-SoXS transmission measurements were performed at beamline 11.0.1.2 [3] at the ALS. Samples for R-SoXS measurements were prepared on a PEDOT: PSS modified Si substrate under the same conditions as used for OSC device fabrication, and then transferred by floating in water to a 1.5 mm × 1.5 mm, 100-nm thick Si_3N_4 membrane supported by a 5 mm × 5 mm, 200 mm thick Si frame (Norcada Inc.). Two dimensional scattering patterns were collected on an in-vacuum CCD camera (Princeton Instrument PI-MTE). The beam size at the sample is 100 μm × 200 μm.

Mobility measurements. Hole-only or electron-only devices were fabricated using the following structures ITO/PEDOT: PSS/donor: FOIC/Au for holes and Al/donor: FOIC/Al for electrons. For hole-only devices, the pre-cleaned ITO glass was spin-coated with PEDOT: PSS (*ca.* 35 nm), then donor: FOIC blend was spin-coated same as photovoltaic devices, then Au (*ca.* 80 nm) was evaporated under vacuum (*ca.* 10^{-5} Pa). For electron-only devices, Al (*ca.* 80 nm) was evaporated onto pre-cleaned glass under vacuum, donor: FOIC blend was spin-coated, then Al (*ca.* 80 nm) was evaporated under vacuum. The mobility was extracted by fitting the current density–voltage curves using space charge limited current (SCLC).[4] The SCLC is described as:

$$J = (9/8)\mu\varepsilon_r\varepsilon_0 V^2 \exp(0.89(V/E_0L)^{0.5})/L^3 \qquad (1)$$

where J is current density, μ is hole or electron mobility, ε_r is relative dielectric constant, ε_0 is permittivity of free space, V is the voltage drop across the device, E_0 is characteristic field, L is the thickness of photovoltaic layer. The thickness of photoactive layer was measured on DektakXT (Bruker).

Transient absorption spectroscopy. TA spectroscopy was carried out using the system described in the literature based on an amplified Ti:Sapphire laser (Spectra-Physics Spitfire).[5, 6] Narrow band ~100-fs excitation (pump) pulses were tuned using a TOPAS-C (light conversion) and chopped at half of the 3-kHz laser rep-rate. Probe pulses spanning the visible to near-IR were generated by focusing 800 nm fundamental laser pulses onto a 3 mm YAG crystal, and the spectrum of every probe shot was recorded. Differential transmission ($\Delta T/T$) spectra were obtained by comparing the average of probe shots with and without excitation. This process was carried out at each time delay, and the final time- and wavelength- dependent TA surface was obtained after averaging 2-4 scans. Films for TA spectroscopy were kept under dynamic vacuum during measurements.

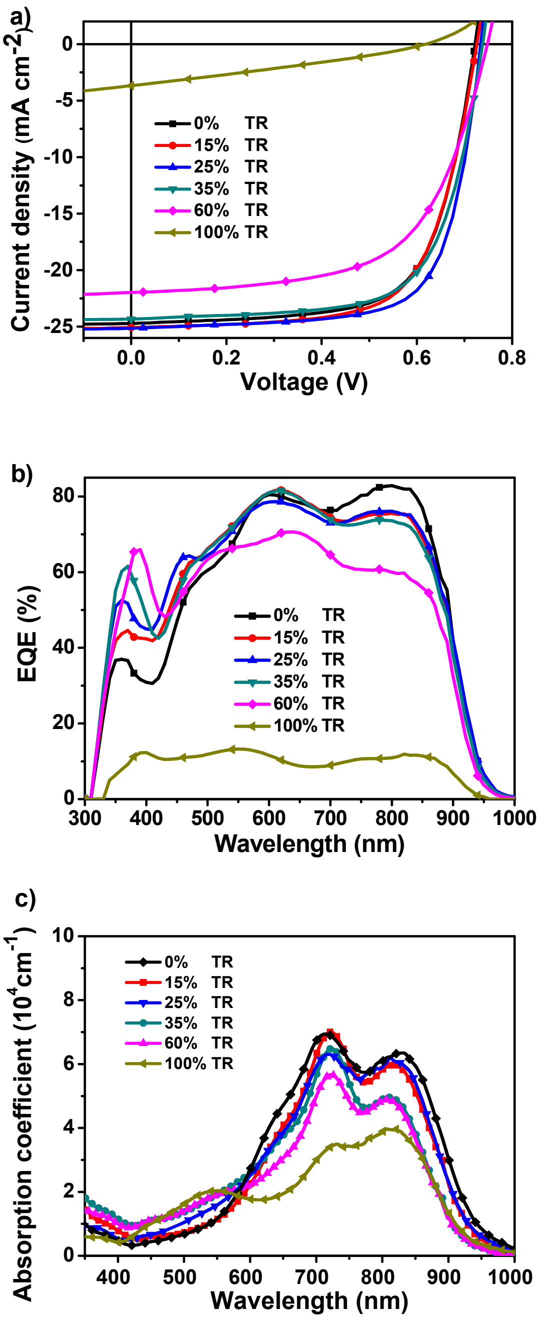

Fig. S1 (a) *J-V* characteristics and (b) EQE spectra of the OSCs based on PTB7-Th/TR/FOIC with different TR weight ratios, (c) absorption spectra of PTB7-Th/TR/FOIC with different TR weight ratios.

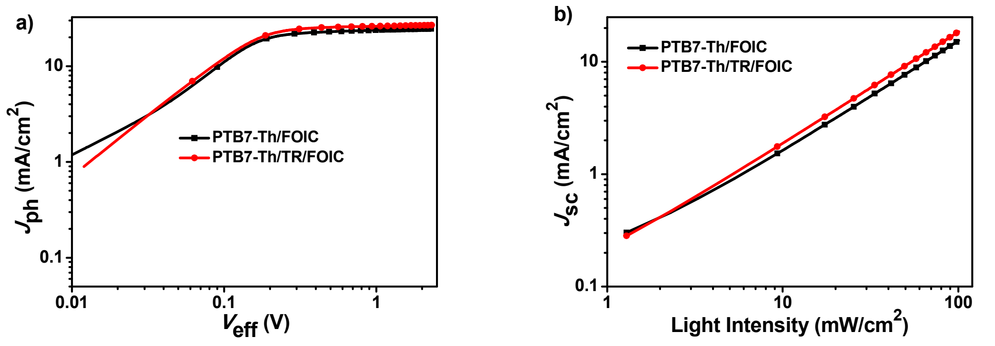

Fig. S2 (a) J_{ph} versus V_{eff} characteristics and (b) J_{sc} versus light intensity of the PTB7-Th/FOIC and PTB7-Th/TR/FOIC blends under optimized condition.

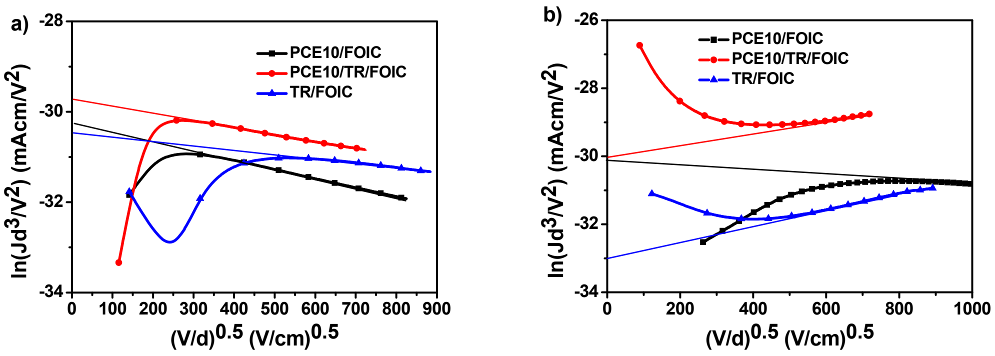

Fig. S3 *J-V* characteristics in the dark for hole-only (a) and electron-only (b) devices based on PTB7-Th/FOIC, TR/FOIC and PTB7-Th/TR/FOIC blends under optimized condition.

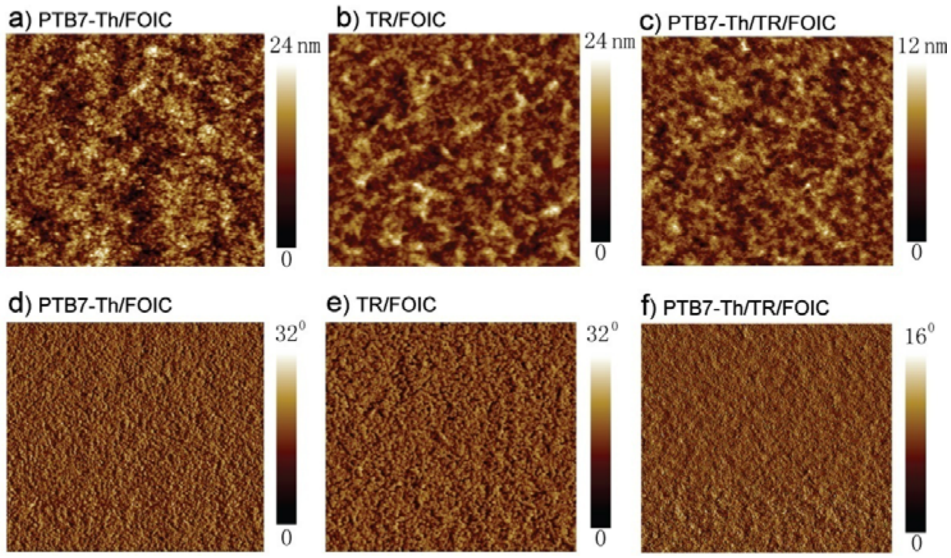

Fig. S4 AFM height (top) and phase (bottom) images of PTB7-Th/FOIC (a and d, R_q = 3.52 nm), TR/FOIC (b and e, R_q = 2.83 nm), PTB7-Th/TR/FOIC (c and f, R_q = 1.41 nm) blends under optimized condition. The scales of images are 3.0 μm × 3.0 μm.

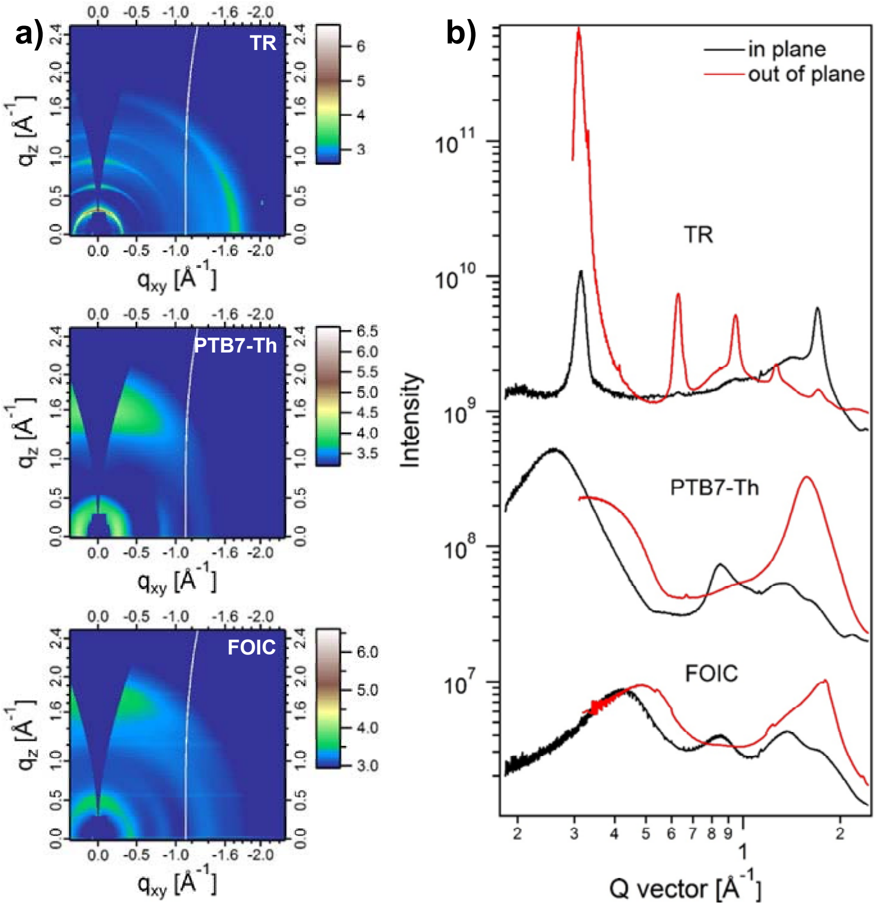

Fig. S5 GIWAXS 2D patterns (a) and 1D line-cuts (b) for TR, PTB7-Th and FOIC neat films.

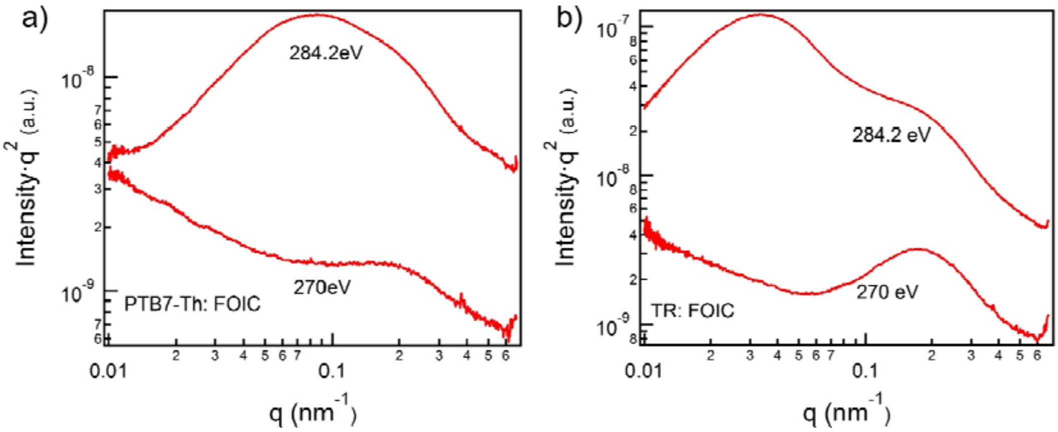

Fig. S6 R-SoXS profiles of (a) PTB7-Th/FOIC and (b) TR/FOIC with the energy of 270 and 284.2 eV.

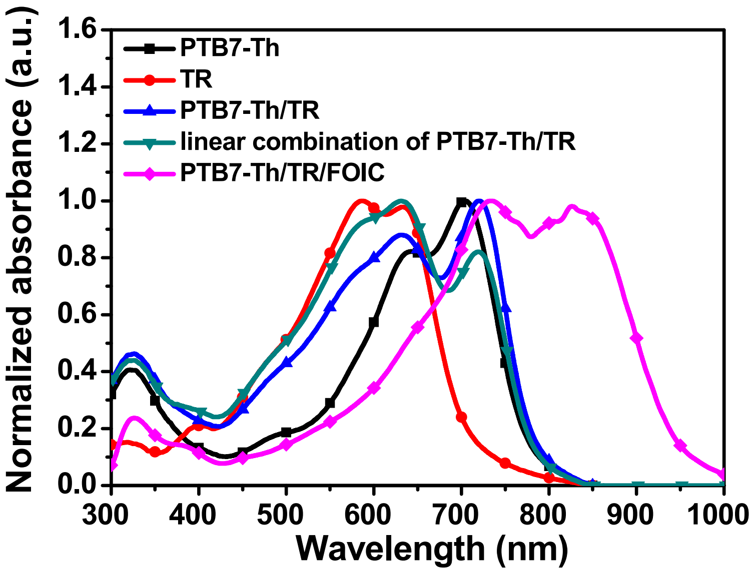

Fig. S7 Absorption spectra of PTB7-Th, TR neat films, PTB7-Th/TR (0.75:0.25, w/w), linear combination of PTB7-Th/TR and PTB7-Th/TR/FOIC (0.75:0.25:1.5, w/w; 0.5% DPE, v/v) blended films.

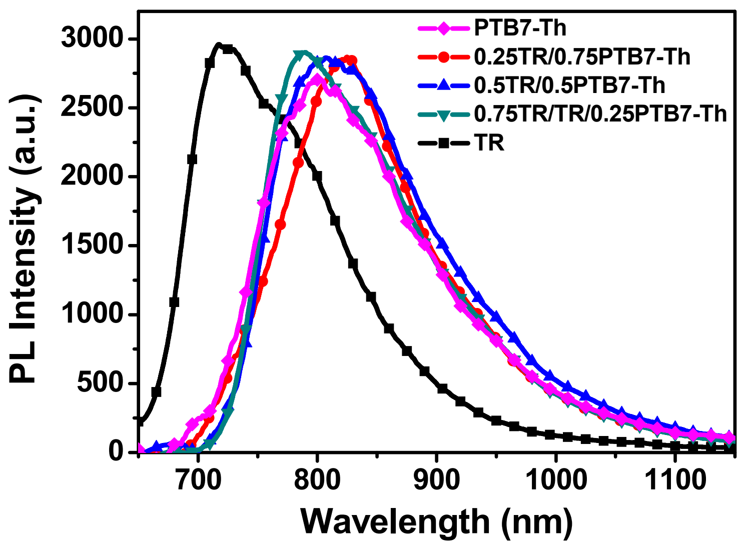

Fig. S8 PL spectra of PTB7-Th, TR neat films and PTB7-Th/TR blended films with different weight ratios (excitation at 500 nm).

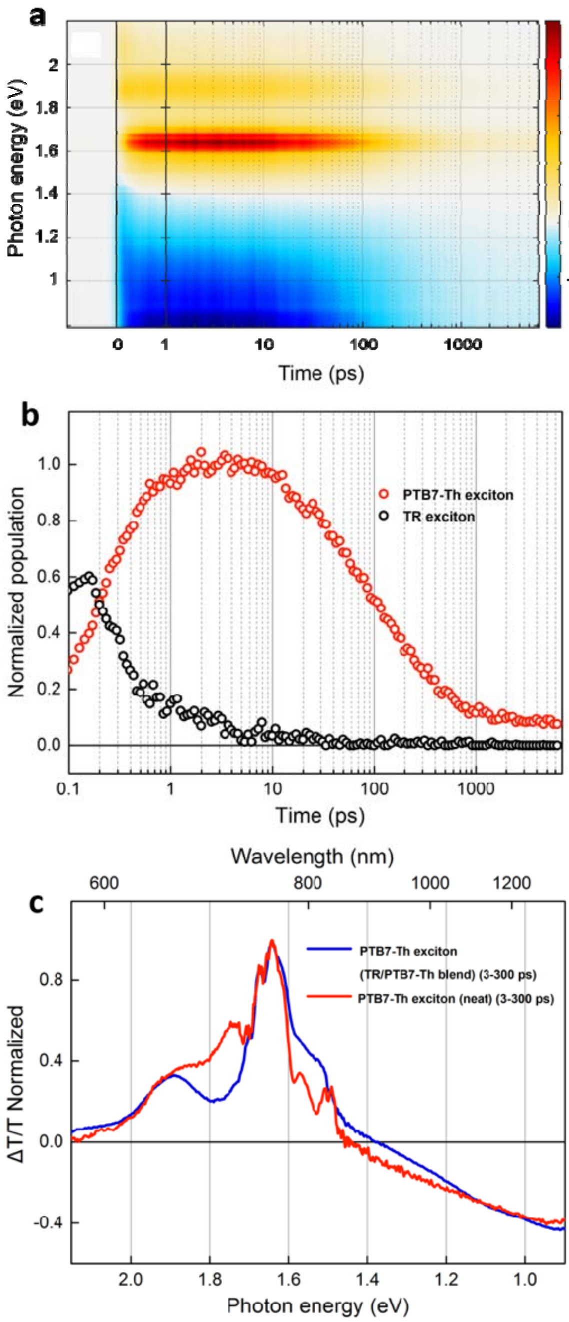

Fig. S9 (a) Transient absorption surface of TR/PTB7-Th blend (excited at 500 nm, pump fluence 3.78 μJ cm^{-2}), (b) energy transfer from TR to PTB7-Th, extracted from a bilinear decomposition of the TR/PTB7-Th blend (excited at 500 nm, pump fluence 3.78 μJ cm^{-2}) and (c) spectra of neat PTB7-Th exciton and TR modulated PTB7-Th exciton.

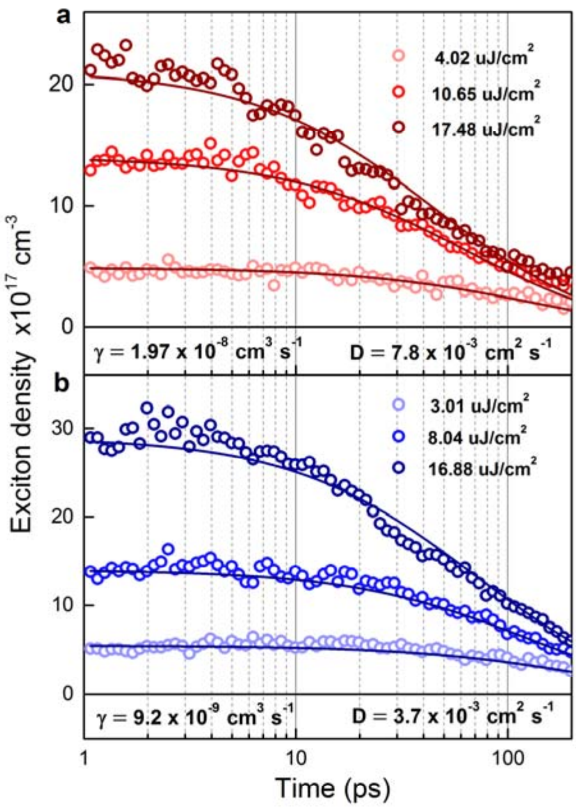

Fig. S10 Exciton-exciton annihilation in (a) neat PTB7-Th and (b) TR/PTB7-Th excitons, and the corresponding annihilation and diffusion constants are noted in the figures. Here, the intensity dependent exciton decays are fitted to the rate equation $\frac{dn(t)}{dt} = -kn(t) - \frac{1}{2}\gamma(t)n^2(t)$, where k is the monomolecular rate constant and γ is the bimolecular rate constant. The 3D diffusion constants are calculated using the equation $D = {}^{\gamma}/_{8\pi R}$ where R is the annihilation radius (assumed to be 1 nm).

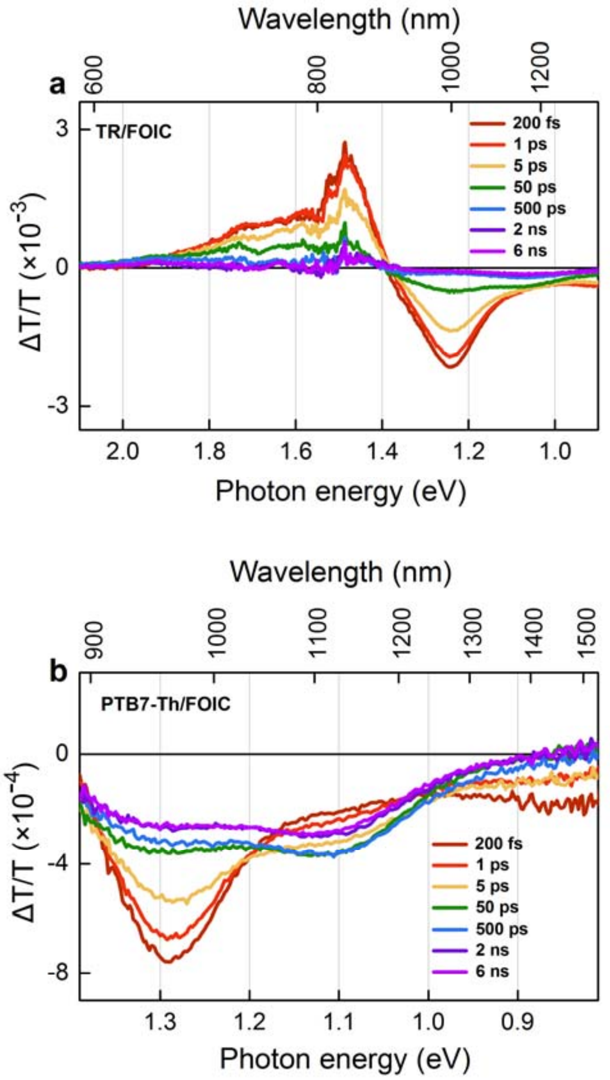

Fig. S11 Series of TA spectra for (a) a binary TR/FOIC film following excitation at 800 nm (1.42 μJ cm^{-2}), and (b) a binary PTB7-Th/FOIC film following excitation at 700 nm (0.6 μJ cm^{-2}).

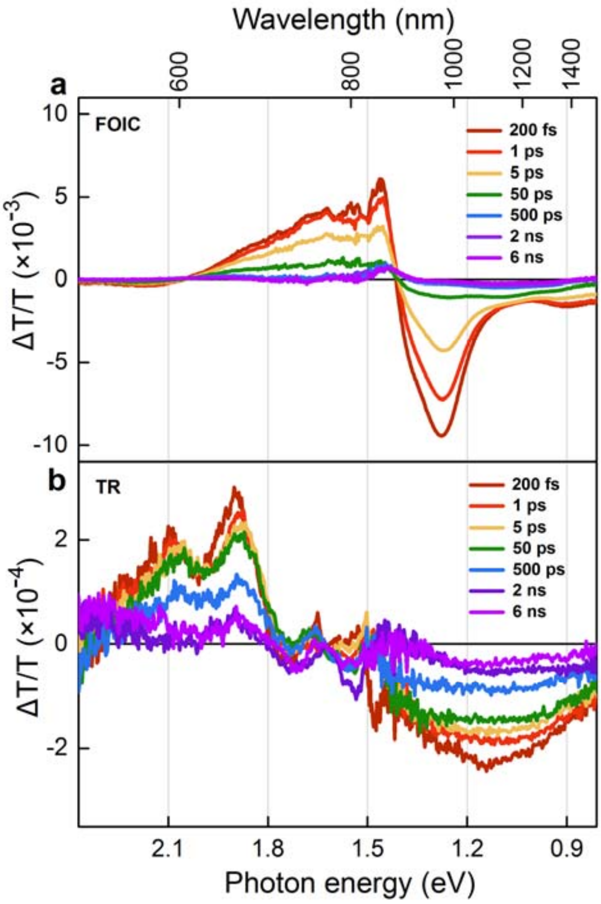

Fig. S12 Series of TA spectra for (a) a neat FOIC film following excitation at 800 nm (4.11 μJ cm^{-2}) and (b) a neat TR film following excitation at 500 nm (0.7 μJ cm^{-2}).

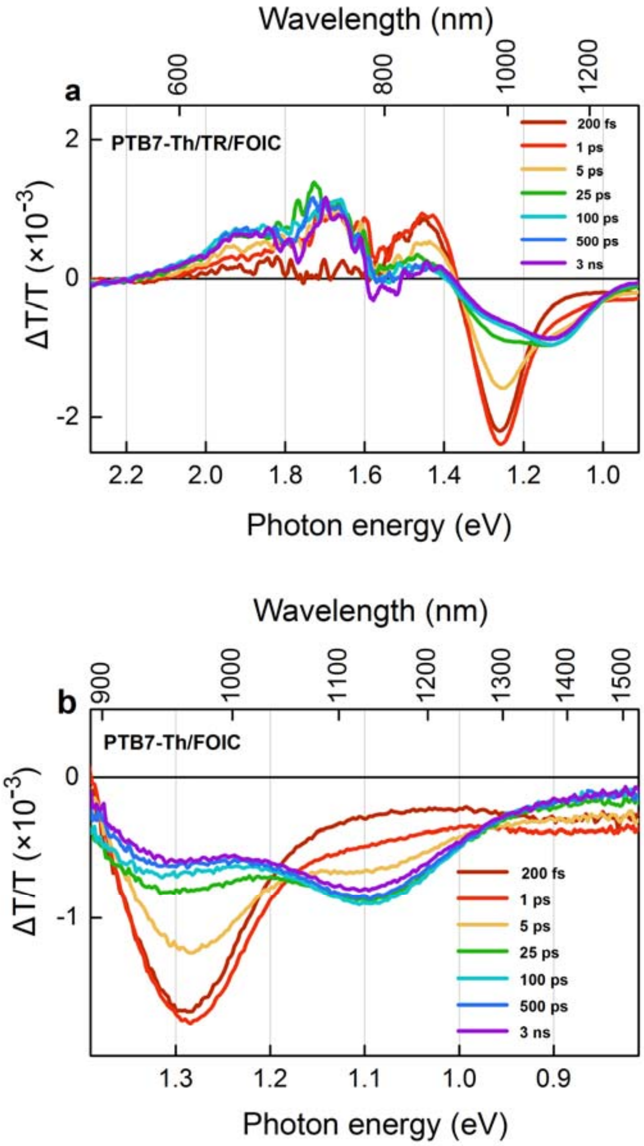

Fig. S13. Series of TA spectra for (a) a ternary PTB7-Th/TR/FOIC film following excitation at 800 nm (0.7 μJ cm^{-2}), and (b) a binary PTB7-Th/FOIC film following excitation at 800 nm (0.58 μJ cm^{-2}). Data in the visible region is poor quality for the ternary blend, and absent in the binary blend, due to low transmission of the probe beam.

Table S1 Performance of the OSCs based on PTB7-Th/FOIC with different DPE ratio [a]

DPE (v/v)	V_{OC} (V)	J_{SC} (mA cm^{-2})	FF (%)	PCE (%)
0	0.742	23.95	66.8	11.9
	(0.737 ± 0.006)	(24.01 ± 0.40)	(65.6 ± 1.4)	(11.6 ± 0.3)
0.5%	0.722	24.73	67.8	12.1
	(0.725±0.003)	(24.62±0.11)	(66.7±1.9)	(11.9±0.2)
1%	0.735	22.87	67.8	11.4
	(0.726±0.012)	(23.19±0.33)	(66.6±1.3)	(11.2±0.2)

[a] Average values (in parenthesis) are obtained from 20 devices.

Table S2 Performance of the ternary OSCs based on PTB7-Th/TR/FOIC with different TR ratio (0.5% DPE)[a]

TR /(TR + PTB7-Th) (%)	V_{OC} (V)	J_{SC} (mA cm^{-2})	calc. J_{SC} (mA cm^{-2})	FF (%)	PCE (%)
0	0.722	24.73	23.96	67.8	12.1
	(0.725±0.003)	(24.62±0.11)		(66.7±1.9)	(11.9±0.2)
15	0.726	25.08	23.98	67.3	12.3
	(0.724±0.004)	(24.79±0.30)		(66.9±0.6)	(12.0±0.3)
25	0.734	25.13	24.00	70.9	13.1
	(0.731±0.003)	(24.97±0.17)		(69.6±1.4)	(12.7±0.4)
35	0.738	24.33	23.77	68.0	12.2
	(0.737±0.005)	(24.10±0.23)		(67.6±1.7)	(12.0±0.2)
60	0.748	21.98	21.02	60.6	10.0
	(0.746±0.003)	(21.90±0.52)		(60.0±1.0)	(9.8±0.2)
100	0.619	3.68	3.67	29.0	0.66
	(0.614±0.006)	(3.25±0.47)		(30.3±2.0)	(0.60±0.1)

[a] Average values (in parenthesis) are obtained from 20 devices.

Table S3 Performance of 75%PTB7-Th/25%TR/FOIC-based devices with different thickness.

thickness (nm)	V_{OC} (V)	J_{SC} (mA cm^{-2})	FF (%)	PCE (%)
80	0.726	24.55	67.1	12.0
100	0.728	24.80	70.0	12.6
110	0.734	25.13	70.9	13.1
140	0.731	25.77	67.2	12.7
180	0.725	25.34	66.5	12.2
200	0.726	25.74	64.0	12.0
300	0.718	24.87	60.7	10.8

Table S4 Hole and electron mobilities of the optimized blends.

blend	μ_h (cm^2 V^{-1} s^{-1})	μ_e (cm^2 V^{-1} s^{-1})	μ_{h}/μ_e
PTB7-Th/FOIC	4.0×10^{-4}	4.8×10^{-4}	0.8
75%PTB7-Th/25%TR/FOIC	6.8×10^{-4}	5.3×10^{-4}	1.3
TR/FOIC	3.4×10^{-4}	2.8×10^{-5}	12.1

References

1 T. Li, S. Dai, Z. Ke, L. Yang, J. Wang, C. Yan, W. Ma and X. Zhan, *Adv. Mater.*, 2017, **30**, 1705969.

2 A. Hexemer, W. Bras, J. Glossinger, E. Schaible, E. Gann, R. Kirian, A. MacDowell, M. Church, B. Rude and H. Padmore, *J. Phys. Conf. Ser.*, 2010, **247**, 012007.

3 E. Gann, A. Young, B. Collins, H. Yan, J. Nasiatka, H. Padmore, H. Ade, A. Hexemer and C. Wang, *Rev. Sci. Instrum.*, 2012, **83**, 045110.

4 G. G. Malliaras, J. R. Salem, P. J. Brock and C. Scott, *Phys. Rev.B.*, 1998, **58**, 13411-13414.

5 J. K. Gallaher, S. K. K. Prasad, M. A. Uddin, T. Kim, J. Y. Kim, H. Y. Woo and J. M. Hodgkiss,

Energy Environ. Sci., 2015, **8**, 2713-2724.

6 A. J. Barker, K. Chen and J. M. Hodgkiss, *J. Am. Chem. Soc.*, 2014, **136**, 12018-12026.